arXiv:0902.4040v2 [astro-ph.SR] 21 Apr 2009

WIYN OPEN CLUSTER STUDY. XXIV. STELLAR RADIAL-VELOCITY MEASUREMENTS IN NGC 6819

K. Tabetha Hole[1,2] (kth@astro.wisc.edu), Aaron M. Geller[1,2] (geller@astro.wisc.edu), Robert D. Mathieu[1,2] (mathieu@astro.wisc.edu), Imants Platais[3] (imants@pha.jhu.edu), Søren Meibom[1,2,4] (smeibom@cfa.harvard.edu), and David W. Latham[4] (dlatham@cfa.harvard.edu)

ABSTRACT

We present the current results from our ongoing radial-velocity survey of the intermediate-age (2.4 Gyr) open cluster NGC 6819. Using both newly observed and other available photometry and astrometry we define a primary target sample of 1454 stars that includes main-sequence, subgiant, giant, and blue straggler stars, spanning a magnitude range of $11 \leq V \leq 16.5$ and an approximate mass range of 1.1 to 1.6 $M_{\odot}$. Our sample covers a 23 arcminute (13 pc) square field of view centered on the cluster. We have measured 6571 radial velocities for an unbiased sample of 1207 stars in the direction of the open cluster NGC 6819, with a single-measurement precision of 0.4 km s^{-1} for most narrow-lined stars. We use our radial-velocity data to calculate membership probabilities for stars with ≥ 3 measurements, providing the first comprehensive membership study of the cluster core that includes stars from the giant branch through the upper main sequence. We identify 480 cluster members. Additionally, we identify velocity-variable systems, all of which are likely hard binaries that dynamically power the cluster. Using our single cluster members, we find a cluster average radial velocity of 2.34 ± 0.05 km s^{-1}. We use our kinematic cluster members to construct a cleaned color-magnitude diagram from which we identify rich giant, subgiant, and blue straggler populations and a well-defined red clump. The cluster displays a morphology near the cluster turnoff clearly indicative of core convective overshoot. Finally, we discuss a few stars of note, one of which is a short-period red-clump binary that we suggest may be the product of a dynamical encounter.

open clusters and associations: individual (NGC 6819); techniques: radial velocities

1. INTRODUCTION

Intermediate-age open clusters (1-5 Gyr), like NGC 6819, provide critical tests for theories of stellar evolution, as these clusters generally display signs of convective core overshoot (i.e., "blue hook" morphologies) at the main-sequence turnoffs. This distinctive morphology is believed to be caused by the rapid contraction of hydrogen-depleted convective cores in stars with masses $M \gtrsim 1.2$ $M_{\odot}$. At the edges of these cores there is a complex interplay between radiative and hydrodynamical processes such that the convective cells can 'overshoot' the classical core edge and mix material to regions outside of the core. The detailed structures of main-sequence turnoffs provide readily available tests of theoretical models of stellar evolution which include convective core overshooting (e.g., Rosvick & Vandenberg 1998, hereafter RV98). Defining the turnoff structure requires excellent photometry, no contamination from field stars, and removal of confusion from the composite light of binaries (e.g., Daniel et al. 1994).

Additionally, studies of open clusters can reveal how stellar dynamics influences pathways in stellar evolution. Blue stragglers are the best-known example, but detailed studies of the 4 Gyr cluster M67 and the 7 Gyr cluster NGC 188 have revealed stars with a variety of non-standard evolutionary paths, including products of dynamical interactions, mass transfer, mergers, etc. (Mathieu & Latham 1986; van den Berg et al. 2001; Mathieu et al. 2003; Sandquist et al. 2003; Geller et al. 2008). Many of these stars and star systems are likely the products of binary encounters leading to stellar exchanges and mergers, and provide a rich array of alternative stellar evolution paths. Again, maximum confidence in membership is required to identify these stars. Both, proper-motion and radial-velocity (RV) membership studies are critical, as photometric determinations of membership by their nature will usually exclude cluster stars with non-standard evolutionary histories.

NGC 6819 has been moderately well studied, yet until now the cluster has lacked a comprehensive kinematic membership study which includes stars from the giant branch through the upper main sequence. There have been multiple photometric studies of NGC 6819 that have helped to define the cluster color-magnitude diagram (CMD) (Burkhead 1971; Lindoff 1972; Auner 1974; Rosvick & Vandenberg 1998; Kalirai et al. 2001). The most recent estimates for the cluster parameters suggest an age between 2.4 and 2.5 Gyr, $(M-m)_V = 12.3$, an E(B-V) between 0.10 and 0.16, and [Fe/H]~ -0.05. Kang & Ann (2002) found evidence for mass segregation in their photometric study of the cluster. Street et al. (2002, 2003, 2005) have discovered numerous photometrically variable stars. Sanders (1972) performed the first and only astrometric membership study, covering a circular area ($r = 18'$) centered on the cluster, and calculated memberships for 189 stars down to $V \sim 14.5$ mag reaching the red giants and blue stragglers. Glushkova et al. (1993), Friel et al. (1989) and Thogersen et al. (1993) performed limited RV studies of the NGC 6819 field, quoting cluster mean RVs that range from +4.8 ± 0.9

---

[1] Astronomy Department, U. Wisconsin-Madison, 475 N Charter St, Madison WI 53706

[2] Visiting Astronomer, Kitt Peak National Observatory, National Optical Astronomy Observatory, which is operated by the Association of Universities for Research in Astronomy (AURA) under cooperative agreement with the National Science Foundation.

[3] Department of Physics and Astronomy, Johns Hopkins University, 3400 North Charles Street, Baltimore MD 21218

[4] Harvard-Smithsonian Center for Astrophysics, 60 Garden Street, Cambridge MA 02138

km s^{-1} to $+1 \pm 6$ km s^{-1}.

The location of NGC6819 in Cygnus places it within the field of view of the Kepler space mission - a search for transiting earth-like planets. Over the planned 4 year mission, Kepler will provide time-series photometric observations with a 30 minute cadence and parts-per-million precision to $V \simeq 17$. Observations by Kepler therefore offer a unique opportunity to study phenomena of stellar photometric variability, and to do so for even Gyr old stars for which such variability can be of very small amplitude. Observations of members of NGC 6819 with Kepler will make possible studies of e.g. stellar rotation and asteroseismology, as well as searches for extra-solar planets and eclipsing binaries, among 2.5 Gyr old stars over a range of masses and evolutionary stages.

We present the first comprehensive high-precision RV survey of the core of NGC 6819 as part of the WIYN Open Cluster Study (WOCS; Mathieu 2000). Our data cover stars from the giant branch through the upper main sequence and include many potential blue stragglers, thereby providing a valuable membership database and the first census of the hard-binary[5] population. First, we present our analysis of all CCD photometry and astrometry of the cluster currently available (§ 2), from which we define our stellar sample (§ 3). We then describe our RV observations, data reduction and precision in § 4. For stars with ≥3 RV measurements, we calculate RV membership probabilities and identify RV variable stars (§ 6). Our data show that NGC 6819 is a rich cluster, with 480 RV selected members in the cluster core with masses in the range of 1.1 to 1.6 $M_{\odot}$. Our RV measurements provide excellent membership discrimination, crucial because of the cluster's location in the Galactic plane. The cleaned CMD (discussed in § 7) reveals rich populations of giants, subgiants and blue stragglers, and a morphology near the cluster turnoff indicative of core convective overshoot. We also identify a few stars of note, including one short-period red-clump binary that we suggest may be the result of a dynamical encounter. Future papers will analyze the dynamical state of the cluster (e.g., mass segregation and velocity dispersion), and study the hard-binary fraction and frequency of orbital parameters.

2. CLUSTER PHOTOMETRY AND COORDINATES

Two primary goals of the WOCS study of NGC 6819 are to provide high-quality *UBVRI* photometry and astrometry. For a preliminary report on the WOCS photometric study see Sarrazine et al. (2003). The astrometric study is underway. Yet to begin our RV survey of the cluster, we required such data in order to define our stellar sample. Thus we conducted a critical analysis of all the photometry and astrometry available to us for use in this paper, and provide the results of this analysis here. We use the 2MASS survey[6] (Skrutskie et al. 2006) as the backbone of this analysis, and define a complete set of 6166 stars in the direction of NGC 6819 within the magnitude range of $11 \leq V \leq 16.5$ and extending to 30 arcminutes from the cluster center. From this set we have selected our stellar sample for the RV survey of the cluster (as explained in § 3.1).

2.1. *Photometry*

There are four sources of CCD *BV* photometry available to us for the cluster: RV98, Kalirai et al. (2001) (hereafter K01), and two unpublished sets taken by members of the WOCS collaboration. (We will use "RV98" and "K01" to refer both to the papers and to the photometry sets used in each, depending on context.) The two sets of WOCS photometry were obtained at what was the KPNO and is now the WIYN[7] 0.9m telescope. In March 1998, C. Dolan and R. Mathieu took *BV* CCD images to begin this RV project, hereafter called Phot98. These observations used the Tektronics CCD (T2KA) at f/7.5, centered on the cluster at $\alpha = 19^{\mathrm{h}}41^{\mathrm{m}}19\overset{\mathrm{s}}{.}3$ (J2000) $\delta = +40^{\circ}11'$, covering a 23′ square (13 pc at 2 kpc distance) field-of-view and a magnitude range of $12.7 < V < 22.0$. The WOCS *UBVRI* study (hereafter Phot03) is based on images obtained with the SITe S2KB CCD camera (pixel size $0\overset{''}{.}60$), yielding a FOV of 20′.

The reductions of the Phot03 CCD frames include the usual bias correction and flat-fielding using sky flats. Standard stars were drawn from the list of Landolt (1992). Instrumental magnitudes were obtained using the DAOPHOT aperture photometry package (Stetson 1987). The photometric calibration equations included zero-point, linear-color, and extinction terms. The Phot98 images were taken on a non-photometric night which precluded applying an absolute calibration. Instrumental magnitudes were calibrated using a zero-point and color-term derived from stars in common between Phot03 and Phot98.

We choose to analyze the zero-points of all the *BV* CCD photometries against Phot03, in the sense 'Δ =target-Phot03'. In all cases only the common stars with $V < 18.5$ are used. By construction, the *BV* system of Phot98 is identical to Phot03. For RV98, we find a mean $\Delta V = -0.002$ and mean $\Delta(B-V) = +0.009$. For K01 the offsets are $\Delta V = +0.018$ and $\Delta(B-V) = +0.004$. The formal uncertainty of the means is 0.004 magnitudes. Considering the high degree of uniformity between the various photometries, when combining *BV* photometries we choose to subtract the offset for only the K01 *V*-magnitudes. All four sets of *BV* photometry are given in Table 1, along with 2MASS *JK* photometry. (Other bands and cross identifications to Sanders and Auner are also provided, where available.) The final *BV* photometry, shown with our RV measurements in Table 2, is derived as the means of all available *V* magnitudes and $(B-V)$ colors. [8]

We note that our *BV* photometry covers a ∼28 arcminute square field of view centered on the cluster center (effectively, the spatial extent of the K01 photometric

---

[5] A hard binary is defined as having an internal energy that is much greater than the energy of the relative motion of a single star moving within the cluster (Heggie 1974). For solar mass stars in a cluster with a one-dimensional velocity dispersion equal to 1 km s^{-1}, all hard binaries have periods less than $\sim 10^5$ days.

[6] This publication makes use of data products from the Two Micron All Sky Survey, which is a joint project of the University of Massachusetts and the Infrared Processing and Analysis Center/California Institute of Technology, funded by the National Aeronautics and Space Administration and the National Science Foundation.

[7] The WIYN Observatory is a joint facility of the University of Wisconsin-Madison, Indiana University, Yale University, and the National Optical Astronomy Observatories.

[8] If there were more than two sets of photometry for a given star, a discordant value was excluded if it exceeded by 3σ the estimated scatter at a given magnitude.

TABLE 1
The first ten lines of the NGC 6819 WOCS photometry database. See §2 for a description of the photometry sources.

WOCS	Phot98				Phot03		RV98		K01		2MASS		Auner	Sanders
ID[a]	V	B-V	V-R	V-I	V	B-V	V	B-V	V	B-V	J	J-K	ID[b]	ID[c]
001001	···	···	···	···	12.692	1.229	12.669	1.245	···	···	10.212	0.929	974	115
002001	13.357	1.248	0.622	1.250	13.399	1.223	13.378	1.238	···	···	10.341	0.722	435	···
003001	13.622	1.194	0.591	1.194	13.664	1.143	13.644	1.164	···	···	11.564	0.673	395	116
004001	13.936	1.203	0.612	1.208	13.994	1.177	13.971	1.191	14.001	1.170	11.847	0.683	428	100
011001	15.701	0.618	0.316	0.719	15.746	0.591	15.720	0.609	15.763	0.600	14.436	0.315	396	···
013001	15.853	0.679	0.392	0.797	15.886	0.689	15.873	0.684	···	···	14.501	0.482	432	···
015001	15.933	0.621	0.334	0.713	15.992	0.607	15.883	0.619	15.969	0.600	14.603	0.378	429	···
001002	···	···	···	···	11.733	1.615	11.837	1.489	···	···	8.819	0.996	550	110
002002	···	···	···	···	12.662	0.379	12.645	0.361	···	···	11.794	0.180	976	105
003002	···	···	···	···	12.760	1.111	12.763	1.130	···	···	10.660	0.736	390	126

[a] See § 2.3 for an explanation of the WOCS ID number.
[b] The ID number from Auner (1974), if available.
[c] The ID number from Sanders (1972), if available.

study) and contains 2724 stars. In 2005, we chose to add additional stars observed by 2MASS to extend our sample to 30 arcminutes in radius from the cluster center (the maximum spatial coverage of the Hydra instrument on the WIYN 3.5m telescope). For these stars, we estimate V magnitudes from 2MASS photometry, using an empirical relationship $V = J + 2.46(J - K) + 0.40$, valid for the region of NGC 6819. To derive this relationship, we used about 850 common stars between 2MASS catalog and Phot03, all brighter than J=15. The standard deviation of the fit is 0.12 mag. This transformation provides a rather crude estimate of V magnitudes. It is used only for 1.7% of stars missing BV photometry over the inner 10x10 arcmin area. In the outer parts of our field, recently added to our survey, the fraction of stars without BV photometry can be as high as 100%. We discuss the development of our stellar sample for the WIYN RV survey in § 3.1.

2.2. *Astrometric Coordinates*

For all four photometric studies, we have also reduced all original pixel data into sky coordinates using the UCAC2 (Zacharias et al. 2004), an accurate, dense, and relatively deep ($r_{lim} \approx 16$) astrometric catalog. All datasets require quadratic and cubic terms in the astrometric plate model. The standard error of astrometric solutions ranges from 50 to 100 mas, with the higher end of the errors attributed to the CFHT 3.6m telescope's CFH12K CCD mosaic data (K01).

We use the 2MASS Point Source Catalog as the primary catalog of stars in the NGC 6819 field, to which we cross-correlate the Phot98, Phot03 and UCAC2 catalogs of photometry and astrometry. In averaging positions, a particular source is excluded only if it shows an offset exceeding 300 mas. The combination of these catalogs provides a comprehensive database for NGC 6819 out to a $30'$ radius, effectively based on the UCAC2 coordinate system. These final coordinates are provided in Table 2. The precision of mean positions is about 30 mas.

2.3. *WOCS Numbering System*

Here we introduce the WOCS numbering system, based on V magnitude and radial distance from the cluster center. Separate one-dimensional Gaussian fits in right ascention (RA) and declination (Dec) to the cluster's apparent density profile (for stars with membership probability $p > 50\%$) provides the following new J2000 center: $\alpha = 19^{\mathrm{h}}41^{\mathrm{m}}17\overset{\mathrm{s}}{.}5$ $\delta = +40^\circ11'47''$. Around this center, annuli of $30''$ width are drawn, and in each ring the stars are sorted in increasing order of their V magnitudes (i.e., the brightest stars have the lowest numbers). If a star is missing a measurement of its V magnitude, it is estimated from the 2MASS catalog using the empirical relationship defined above. The identification number (ID) is the three digit star number followed by the three digit annulus number, (e.g., the star 001003 is the brightest star in the third annulus).[9]

3. STELLAR SAMPLE FOR THE RADIAL-VELOCITY SURVEY

To improve observational efficiency, previous RV surveys of open clusters have often pre-selected their target stars with preference to proper-motion members. Unfortunately, NGC 6819 lacks a complete proper-motion database from which we can efficiently prioritize our sample. For a rich cluster in the Galactic plane, such as NGC 6819, the observational requirements for a complete, unbiased RV survey are particularly daunting. However, the capabilities of modern multi-object spectrographs have grown to such a degree that we have been able to measure RVs for a large sample of stars in the field of NGC 6819 in the absence of measured proper motions. Our full NGC 6819 RV database is the combination of a WIYN and a CfA data set; we describe the respective stellar samples below.

3.1. *WIYN*

When we began our WIYN RV survey of NGC 6819 in 1998, we used the photometry from RV98 and Phot98 to compile our "primary sample". Thus this sample of stars is limited in spatial extent to the 23 arcminute field-of-view of the Phot98 observations. Our RV observations are most complete within the primary sample (see § 5.1), as we have only recently extended our survey to include additional stars observed in subsequent photometric studies. In the following section, we describe the

---

[9] We note that the V magnitude used to order the stars is not the final catalog V magnitude, which was derived at a later stage of reductions. Thus the sequence may not be precisely consistent with the photometry.

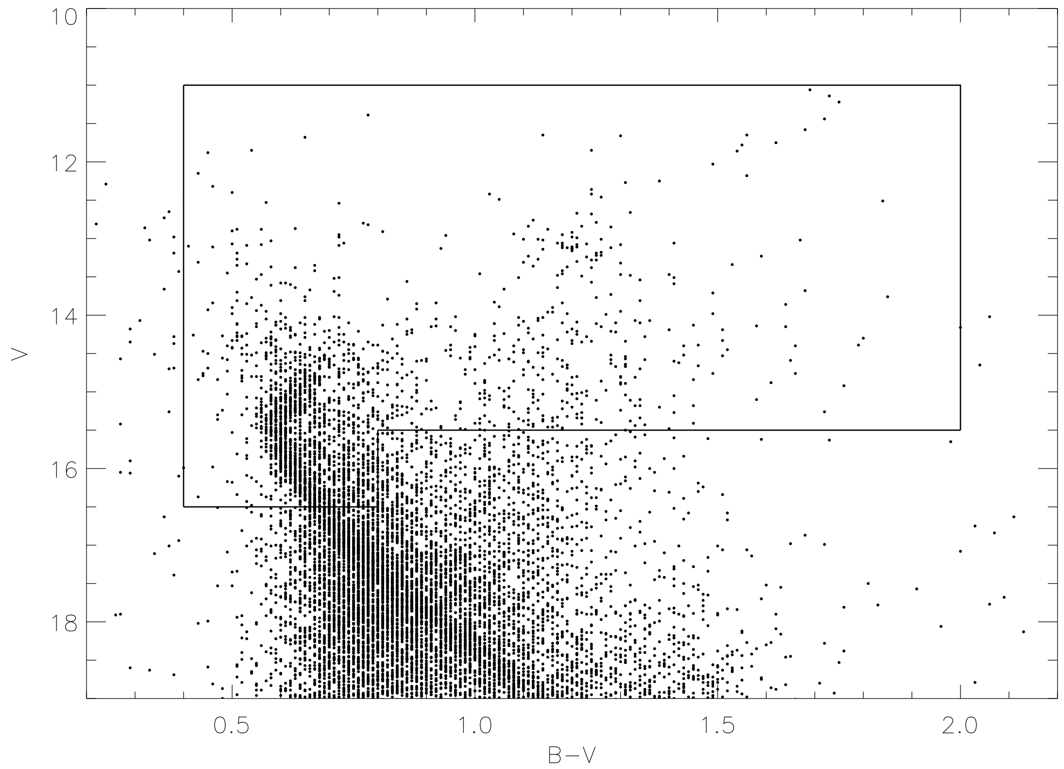

FIG. 1.— CMD displaying all stars in a 30-arcminute-radius field around NGC 6819. The outlined region designates the photometric limits of our primary WIYN stellar sample.

development of our stellar sample over the ∼10 years of our RV survey.

Our selection for the WIYN primary sample was influenced by the instrument used for the study, the Hydra Multi-Object Spectrograph (MOS) on the WIYN 3.5 m telescope on Kitt Peak (Barden et al. 1994). The Hydra MOS has an effective dynamic range of roughly four magnitudes within a given configuration of fibers, or a "pointing"; sources more than four magnitudes fainter than the brightest are vulnerable to contamination by scattered light in the spectrograph. The faintest sources that Hydra MOS can observe efficiently at high spectral resolution are $V \sim 16.5$ mag; this therefore sets our faint limit in magnitude. At colors bluer than $(B-V)$ ∼0.4 (or $(B-V)_o \sim 0.2$ mag using the $E(B-V) = 0.16$ mag found by RV98), lower line densities and increased line widths, typical of earlier-type stars, make deriving reliable RV measurements increasingly difficult. Therefore our blue limit in color is set by astrophysical constraints.

We therefore chose to define our WIYN primary sample to cover the magnitude range of $11 \leq V \leq 15.5$ within the color range of $0.4 \leq (B-V) \leq 2.0$, with an additional magnitude range of $15.5 \leq V \leq 16.5$ within the color range of $0.4 \leq (B-V) \leq 0.8$. Our photometric selection criteria are shown in the CMD of Figure 1. The reduced color range for stars on the fainter end is designed to concentrate attention on the main sequence at magnitudes below the cluster turnoff and subgiant branch. As our primary sample was originally compiled from the Phot98 photometric study, this sample covers the same 23 arcminute square field-of-view. The primary sample contains 1454 stars, covering the upper main sequence through the turnoff region and the giant branch, including the red clump, as well as most potential blue stragglers. This initial list of target stars has since been increased by the addition of subsequent photometric studies and 2MASS sources within our magnitude range (as described in § 2). However, our observations are most complete within the primary sample, and, as such, most of the results presented in the paper are derived from this sample.

3.2. *CfA*

Mathieu and Latham began observations of NGC 6819 to measure RVs at the Harvard-Smithsonian Center for Astrophysics facilities in 1988. A sample of 191 stars were selected from the proper-motion study of Sanders (1972) and the photometric survey of Auner (1974). Given the effective magnitude limit of the CfA Digital Speedometers, that study was only able to reach the top of the main sequence. 170 of these 191 stars are within the WOCS primary sample. The remainder are generally brighter than $V = 11.0$ mag, bluer than $(B-V) = 0.4$, or have incomplete photometry.

4. RADIAL-VELOCITY OBSERVATIONS, DATA REDUCTION AND PRECISION

4.1. *WIYN*

The Hydra MOS is a fiber-fed spectrograph with a one-degree field of view, currently capable of taking ∼80 simultaneous spectra, with an effective dynamic range of roughly four magnitudes within a given pointing. In total, we have observed 90 pointings on NGC 6819 over 35 separate observing runs on the WIYN 3.5m.

Developing a strategy for prioritizing the stars in our sample for placement of the ∼80 fibers during each pointing is critical to optimizing limited observing time. In order to satisfy the four-magnitude dynamic range, we first define a faint sample, covering the magnitude range of $12.5 \leq V \leq 16.5$, to be observed in good weather conditions. We also developed a bright sample, covering the magnitude range of $11 \leq V \leq 15$, to be observed in the case when light cloud cover would likely prevent us from deriving reliable RVs for fainter stars. Our original strategy for observations gave highest priority to stars within 200″ (∼2 pc) from the cluster center; within that radius, targets were prioritized by brightness. Outside 200″, where membership probability decreases significantly with radius, sources were prioritized by radius from the cluster center.

As our survey matured, we adopted a more sophisticated strategy for prioritizing the stars in our observing lists (both faint and bright). Monte Carlo simulations show that we require at least three observations over the course of a year to ensure 95% confidence that a star is either constant or variable in velocity (Mathieu 1983). Given three observations with consistent velocity measurements over a timespan of at least a year and typically longer, we classify a given star as single (strictly, non-velocity variable) and finished, and move it to the lowest priority. If a given star has three RV measurements with a standard deviation >1.6 km s^{-1} (four times our precision; see § 6.2), we classify the star as velocity variable and give it the highest priority for observation on a schedule appropriate to its timescale of variability. This prioritization allows us to most efficiently derive orbital solutions for our detected binaries. We have made a strong effort to observe all stars in our primary sample with $V \leq 15$ at least three times, and have therefore prioritized these stars in our observations. These stars span the giant branch through the upper-main sequence and contain most potential blue stragglers. There are 436 stars within our primary sample with $V \leq 15$.

We place our shortest period binaries at the highest priority for observations each night, followed by longer period binaries to obtain 1-2 observations per run. Below the confirmed binaries we place, in the following order, "candidate binaries" (once-observed stars with a radial-velocity measurement outside the cluster radial-velocity distribution or stars with a few measurements that span only 1.5-2 km s^{-1}), once observed and then twice observed non-velocity-variable likely members, twice observed non-velocity-variable likely non-members, unobserved stars, and finally, "finished" stars. Within each group, we prioritize by distance from the cluster center, giving those stars nearest to the center the highest priority.

Our observing procedure and data reduction process for WOCS RV observations are described in detail in Geller et al. (2008). Briefly, we use the echelle grating, providing a spectral resolution of roughly 15 km s^{-1}. The majority of our spectra are centered at 513.0 nm with a range of 25 nm, covering numerous narrow absorption lines including the Mg I b triplet. During data reduction, the images are bias- and sky-subtracted, and the extracted spectra are flat fielded, throughput corrected, and dispersion corrected. The WIYN spectra have signal-to-noise ratios ranging from ∼18 per resolution element for V=16.5 stars to ∼120 per resolution element for V=12.5 stars in a two-hour exposure. The RVs are derived from a one-dimensional cross-correlation with an observed solar template spectrum, corrected to be at rest (e.g., Tonry & Davis 1979). We performed a detailed study of the effect of using the solar template across our $(B-V)$ color range in Geller et al. (2008), finding no noticable systematic offset (given our precision of 0.4 km s^{-1}). These RVs are then converted to heliocentric RVs and are corrected for the unique fiber offsets of the Hydra MOS.

We have analyzed the precision of our WIYN NGC 6819 RV measurements in the same method as in Geller et al. (2008), following the process described in Kirillova & Pavlovskaya (1963). A χ^2 function fit to the distribution of standard deviations of our NGC 6819 WIYN RV measurements yields a precision for our WIYN data of 0.4 km s^{-1} for a single observation, the same value found in Geller et al. (2008).

4.2. *CfA*

The CfA RV measurements were obtained with two nearly identical instruments on the Multiple Mirror Telescope[10] and the 1.5-m Tillinghast Reflector at the Whipple Observatory atop Mt. Hopkins, Arizona (Latham 1992). Echelle spectrographs were used with intensified photon-counting Reticon detectors to record about 4.5 nm of spectrum in a single order near 518.7 nm, with a resolution of 8.3 km s^{-1} and signal-to-noise ratios ranging from 8 to 15 per resolution element. Information on the CfA data reduction process can be found in Stefanik et al. (1999).

A χ^2 analysis of the CfA precision yields a value of ~ 0.7 km s^{-1}. This value agrees well with that derived by Mathieu et al. (1986) for CfA RVs from stars in M67.

5. THE COMBINED WIYN AND CFA RADIAL-VELOCITY DATA SET

The majority of our observations, 5455 measurements of 1102 stars, were taken with the WIYN Hydra MOS, starting in June 1998 and still ongoing. The WIYN measurements have a typical frequency of ∼four epochs per year. Additionally, we have 733 CfA measurements of 170 stars. The bulk of the CfA measurements were taken from May 1988 through October 1992, though some were taken through 1995. The CfA measurements have a typical frequency of ∼five epochs per year.

Prior to combining the WIYN and CfA data sets, we first searched for a potential zero-point offset by comparing stars with ≥ 3 measurements in each sample and with a standard deviation of ≤ 1.0 km s^{-1}. There are 15 such stars common to both the WIYN and CfA samples. One of these stars has a difference in average velocities of 23 km s^{-1} and was removed from the comparison. For the remaining stars, the mean offset between the WIYN and the CfA average velocities is 0.07 km s^{-1}, less than the standard deviation of the mean of the difference (0.11 km s^{-1}). As stated above, the precision on our WIYN measurements is 0.4 km s^{-1}, and the precision on our CfA measurements is approximately twice that, at 0.7 km s^{-1}. Thus, we conclude that there is no

---

[10] The Multiple Mirror Telescope is a joint facility of the Smithsonian Institution and the University of Arizona.

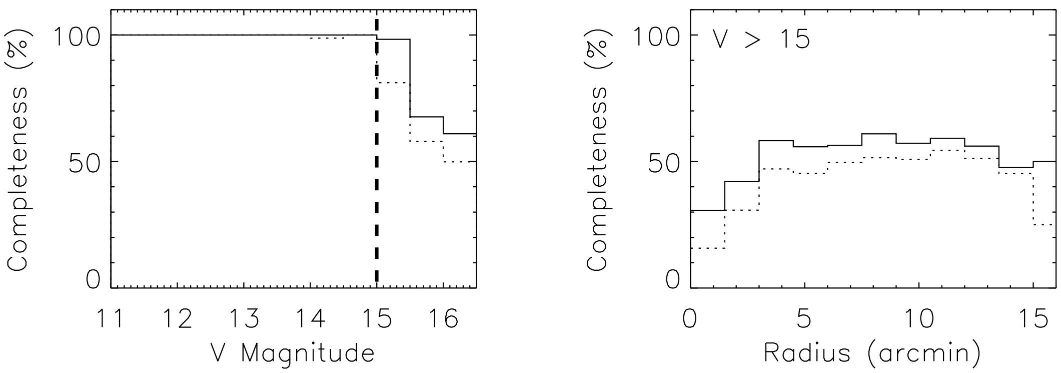

FIG. 2.— Completeness histograms of observed stars in our NGC 6819 primary sample. For both plots, we use the solid and dashed lines to indicate the completeness in stars with ≥1 and ≥3 radial-velocity measurements, respectively. On the left, we show the completeness as a function of V magnitude. We are essentially complete for all stars with $V \leq 15$, as indicated by the dashed line. On the right, we show the completeness for stars with $V > 15$, essentially plotting our completeness amongst the main sequence stars in our sample, as a function of radius from the cluster center.

significant zero-point offset between the two data sets at the level of our precision, and we therefore combine the WIYN and CfA data without modification. When using the measurements in our analyses, such as RV averages, they are weighted by the inverse of their respective precisions (see Equation 5). We note that the CfA data significantly increase our time baseline with which to detect and find orbital solutions for long-period binaries.

5.1. *Completeness Within the Primary Sample*

Of the 1454 stars in our primary sample (see § 3.1) we have at least one RV measurement of 1207 targets (83%). Over half of the stars in this primary sample have sufficient measurements for their RVs to be considered final (924 of 1454, 64%). This means that for each of these stars we have at least three velocity measurements that are consistent, or if they are variable, that we have found binary orbital solutions (discussed in §6.2). Of those stars not finalized, 130 stars have only one or two observations and another 153 stars are variable but do not yet have definitive orbital solutions. Because of our emphasis on the brighter (i.e. more evolved) stars (§4), we have final measurements for 386 of the 436 stars in the primary WIYN sample with $V \leq 15.0$ mag, for a completeness of 89%. Forty eight of the remaining 50 stars are velocity variables (including some rapidly rotating stars) without orbital solutions yet.

In Figure 2 we plot the completeness in our primary sample as a function of both V magnitude (left) and projected radius (right). We plot the completeness in stars observed ≥3 times with the dashed line, and stars observed ≥1 time with the solid line. A targeted effort has been made to ensure that our observations for this sample are nearly complete down to V=15; there are only two stars that have less than three observations in this bright sample. Both are rotating too rapidly to derive reliable RVs with our current observating setup. Towards fainter magnitudes, the completeness drops to ∼60% at V=16.5. These fainter stars require clear, dark skies in order to derive reliable RV measurements, and there is a very large increase in the number of stars in our primary sample as we begin to include the main sequence (Figure 1).

Further, crowding limits for the Hydra MOS fibers and the high surface density of main sequence stars near the cluster center make it more challenging to obtain the same completeness in this region. This can be seen in Figure 2 showing completeness as a function of radius for (largely) main-sequence stars.

6. RESULTS

Our full NGC 6819 database is available with the electronic version of this paper; here we show a sample of our results in Table 2. For each star, we list the WOCS identification number, right ascension (α), declination (δ), the averaged BV photometry (see §2), number of RV measurements, the mean and standard error of the RV measurements, the e/i value (see § 6.2), the calculated RV membership probability (see § 6.1), and the classification of the object (see § 6.3). For velocity-variable stars with orbital solutions, we present the center-of-mass (γ) RV and its standard error, and add the comment SB1 or SB2 for single- and double-lined binaries, respectively.

6.1. *Radial-Velocity Membership Probabilities*

NGC 6819 lies close to the plane of the Galaxy ($\ell = 74^{\circ}.0$ $b = +8^{\circ}.5$), and the cluster RV distribution is embedded within the field velocity distribution. Even so, in a histogram of the RVs of single stars, the cluster population is readily distinguishable from the bulk of the field stars (Figure 3). The cluster can be seen as the tightly peaked velocity distribution ($\sigma \sim 1.0$ km s^{-1}) centered around a mean velocity of 2.3 km s^{-1}. In order to calculate RV membership probabilities for each star, we simultaneously fit one-dimensional Gaussian functions $F_c(v)$ and $F_f(v)$ to the cluster and field RV distributions respectively. We then compute membership probability $p(v)$ with the usual formula:

$$p(v) = \frac{F_c(v)}{F_f(v) + F_c(v)} \tag{1}$$

(Vasilevskis et al. 1958) (see Table 3 for fit parameters). We use only single stars in computing the Gaussian fits. The RV distribution and the Gaussian fits are shown in Figure 3.

For single stars, we use the mean RVs in Table 2 to compute membership probabilities. For binary stars with orbit solutions, we compute membership probabilities

TABLE 2
The first ten lines of the NGC 6819 WOCS radial-velocity database. Coordinates are in J2000. The radial velocity given is the mean of the measurements. For binaries with solutions, we include the center-of-mass velocity γ and any comments about the nature of the system. The standard error of the mean is also given. If we only have a single measurement, the WIYN or CfA measurement precision is given instead, as appropriate. For binaries with orbital solutions, we provide the error on γ from the orbital fit in this column instead.

WOCS ID[a]	α	δ	V	B-V	N_{WIYN}	N_{CfA}	$\overline{RV}$	Std. Err.	e / i	Mem. Prob.	Class[b]	γ	Comment
001001	19 41 18.71	40 11 42.9	12.68	1.24	3	20	6.04	3.40	23.88	···	BU	···	···
002001	19 41 18.93	40 11 41.0	13.38	1.24	3	0	0.94	0.04	0.13	88	SM	···	···
003001	19 41 18.76	40 11 54.8	13.64	1.17	4	2	1.42	0.30	1.29	93	SM	···	···
004001	19 41 15.75	40 11 36.0	13.98	1.19	3	5	1.49	0.18	0.77	93	SM	···	···
005001	19 41 16.21	40 11 26.4	15.02	0.64	1	0	4.90	0.4	···	···	U	···	···
006001	19 41 18.25	40 11 34.8	15.20	0.61	2	0	-0.93	1.87	···	···	U	···	···
007001	19 41 17.27	40 11 27.3	15.20	0.65	3	0	2.24	0.28	1.00	95	SM	···	···
008001	19 41 18.63	40 11 35.2	15.27	0.61	3	0	2.16	2.27	8.04	···	BLM	···	···
009001	19 41 18.01	40 11 19.6	15.48	0.61	1	0	5.66	0.4	···	···	U	···	···
011001	19 41 16.51	40 11 53.4	15.73	0.60	1	0	3.73	0.4	···	···	U	···	···

[a] See § 2.3 for an explanation of the WOCS ID number.
[b] See § 6.3 for an explanation of the class codes.

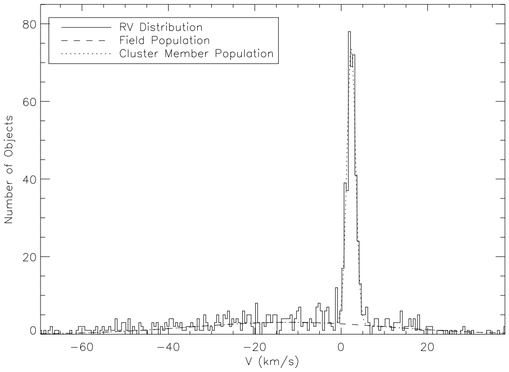

Fig. 3.— RV distribution of single stars with ≥3 RV measurements. The cluster population is clearly distinguishable from the field distribution as the tightly peaked distribution centered on 2.3 km s^{-1}.

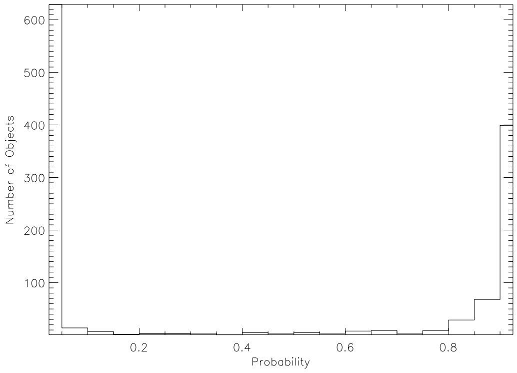

Fig. 4.— RV membership probabilities for single stars with ≥3 RV measurements in the field of view of NGC 6819. The probabilities display a clean separation between cluster and field stars. We classify as cluster members those stars with a RV membership probability $p \geq 50\%$.

TABLE 3
Gaussian Fit Parameters For Cluster and Field RV Distributions

	Cluster	Field
Ampl. (Number)	58.3 ± 1.0	3.1 ± 0.3
$\overline{RV}$ (km s^{-1})	2.338 ± 0.019	-12.0 ± 1.8
σ (km s^{-1})	1.009 ± 0.019	23 ± 3

from the γ velocity. For velocity-variable stars without orbit solutions, the γ-velocities are not known, and therefore we cannot calculate an RV membership. For these stars, we provide a preliminary membership classification, described in § 6.3.

The probability distribution in Figure 4 shows a very clean separation of cluster members and field stars. In the following analysis, we use a probability cutoff of $p \geq 50\%$ for classification as a member. This criterion for membership gives 397 single cluster members. Using only these single members, we find a mean cluster velocity of 2.34 ± 0.05 km s^{-1}. From the area under the fit to the cluster and field distributions, we expect 364 single cluster members as well as 33 field stars having velocities that result in $p \geq 50\%$. Thus we estimate a field contamination of 9%. Though this estimate is derived from single stars, the percent contamination should be valid for the cluster as a whole.

6.2. *Velocity-Variable Stars*

Velocity-variable stars are distinguishable by the larger standard deviations of their RV measurements. Here, we assume that such velocity variability is the result of a binary companion (or perhaps multiple companions). Specifically, we consider a star to be a velocity-variable if the ratio of the standard deviation of its RV measurements to our measurement precision is greater than four (Geller et al. 2008). We refer to this ratio as e/i, where "e" is the standard deviation of the RV measurements for the star, and "i" is our measurement precision. As stated in § 4 we find a precision for the WIYN data of 0.4 km s^{-1} while the CfA data have a precision of 0.7 km s^{-1}. For stars with multiple RV measurements from both observatories, our combined e/i value is weighted by the expected precision of each measurement. From Bevington & Robinson (1992), the variance for a data set with multiple precision values is defined as

$$e^2 = \frac{N}{N-1}\frac{\sum_i^N (RV_i - \bar{RV})^2/\sigma_i^2}{\sum_i^N 1/\sigma_i^2}. \tag{2}$$

The square of the expected precision for this data set is defined as

$$i^2 = \frac{1}{N}\sum_i^N \sigma_i^2. \tag{3}$$

Thus the e/i value for stars with multiple RV measurements from both observatories is given by

$$\left(\frac{e}{i}\right)^2 = \frac{N^2}{N-1}\frac{\sum_i^N (RV_i - \bar{RV})^2/\sigma_i^2}{\sum_i^N \sigma_i^2 \sum_i^N 1/\sigma_i^2} \tag{4}$$

where the $\bar{RV}$ is the mean RV weighted by the respective precision values, and is defined as,

$$\bar{RV} = \frac{\sum_i^N (RV_i/\sigma_i^2)}{\sum_i^N (1/\sigma_i^2)}. \tag{5}$$

Again, σ_i is 0.4 km s^{-1} for WIYN measurements and 0.7 km s^{-1} for CfA measurements.

In this manner, we can calculate reliable e/i values for narrow-lined stars. Stars with e/i<4 are labelled as single; however, certainly some fraction of these stars are long-period and/or low-amplitude binaries. For double-lined binaries and rapidly-rotating stars, however, the precision on our measurements is less well defined. We do not derive an e/i value for such stars. In the case of double-lined spectra, we take their multiplicity as given and label them as velocity variables directly (providing the comment of SB2 in Table 2).

To date, we have identified 205 velocity variables. We have derived orbital solutions for 52 of these. 41 of the resulting gamma velocities give $p \geq 50\%$ and are thus likely to be cluster members. For the binaries with orbital solutions, we quote the γ-velocities in Table 2. In following papers, we will provide the full orbital solutions including all derived parameters for each binary, as well as detailed analyses of the distributions of orbital parameters and the binary frequency of the cluster.

6.3. *Membership and Variability Classification*

In addition to our RV membership probabilities and e/i measurements, we also provide a qualitative classification for each narrow-lined star observed ≥3 times as a guide to its membership and variability. Again, we consider a star to be single if its e/i<4. For these stars we classify those with $p \geq 50\%$ as single members (SM), and those with $p < 50\%$ as single non-members (SN). If a star has e/i≥4 and enough measurements from which we are able to derive an orbital solution, we use the γ-velocity to compute a secure membership. For these binaries, we classify those with $p \geq 50\%$ as binary members (BM) and those with $p < 50\%$ as binary non-members (BN). For velocity variables without orbital solutions, we split our classifications into three categories. If the mean RV results in $p \geq 50\%$, we classify the system as a binary likely member (BLM). If the mean RV results in $p < 50\%$ but the range of measured velocities includes the cluster mean velocity, we classify the system as a binary with unknown membership (BU). Finally, if the RV measurements for a given star all lie either at a lower or higher RV than the cluster distribution, we classify the system as a binary likely non-member (BLN), since it is unlikely that any orbital solution could place the star within the cluster distribution. We classify stars with <3 RV measurements as well as some rapid rotators as unknown (U), as these stars do not meet our minimum criterion for deriving RV memberships or e/i measurements. In the following analysis, we include the SM, BM and BLM stars as cluster members. We list the number of stars within each class in Table 4. The total number of cluster members in our sample is 480.

TABLE 4
NUMBER OF STARS WITHIN EACH CLASSIFICATION

Classification	N Stars
SM	397
SN	475
BM	41
BN	11
BLM	42
BLN	69
BU	42
U	130

7. DISCUSSION

7.1. *Color-Magnitude Diagram*

The ability of our RV survey to distinguish between members of NGC 6819 and the field is evident in a comparison of the two CMDs shown in Figure 5. The upper CMD includes all stars for which we have RV measurements, while the lower CMD includes only RV-selected cluster members (i.e., SM, BM and BLM stars). In the latter, the classic cluster sequence is revealed from the upper main sequence through the red clump. We plot the velocity variables with triangles and the single stars with circles. Note the rich giant, subgiant and blue straggler populations as well as the large number of detected binaries.

In Figure 6 we again present the CMD with only kinematically-selected, single cluster members. In this figure we also plot a Marigo et al. (2008) isochrone model, which includes core convective overshoot. The displayed isochrone was created using cluster age of 2.4 Gyr and solar metallicity, which are consistent with the range of cluster parameters determined by different groups for NGC 6819. The isochrone was placed by eye, using $(m-M) = 12.3$ mag and $E(B-V) = 0.1$ mag. With this isochrone the cluster turnoff is found to be at $\sim 1.53\ M_\odot$.

There is mounting evidence that the Schwarzschild cri-

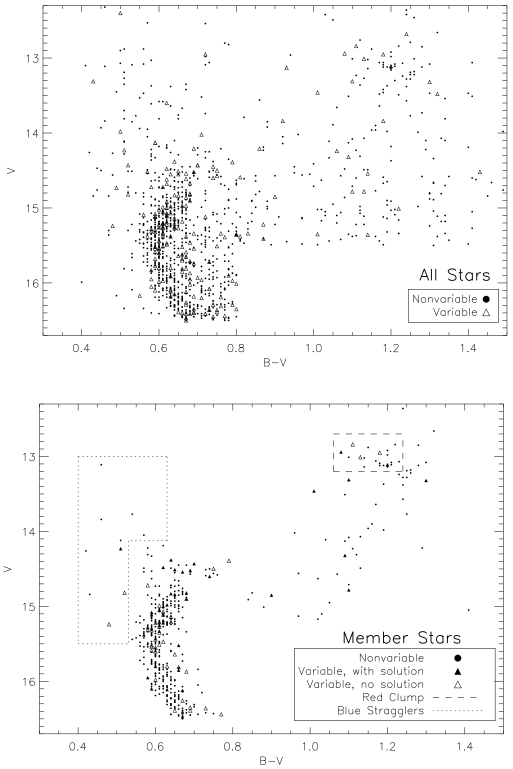

FIG. 5.— Color-magnitude diagram of all stars with WOCS RV measurements (top) and RV-selected narrow-lined member stars (bottom). The triangles in the upper diagram represent velocity variables. The filled triangles in the lower (cluster member) diagram are binaries with orbital solutions (BM). Open triangles are velocity variables currently without solutions but with mean velocities indicating membership (BLM). The color and magnitude criteria used for identifying the red clump and blue straggler populations are also indicated with the dotted and dashed lines, respectively.

terion ($\nabla_{ad} \geq \nabla_{rad}$) underestimates the size of the convective core of intermediate mass stars, most likely due to effects of turbulence and rotation at the convective-radiative boundary (e.g., Shaviv & Salpeter 1973; Zahn 2002). This provides extra fuel to the hydrogen-burning core and increases the star's main sequence lifetime, as well as the eventual size of the hydrogen-depleted region when core fusion ceases. As the star leaves the main sequence, the core begins to contract, the temperature in the outer layers increases and eventually hydrogen fusion ignites in a shell around the depleted core. Because the depleted region is larger in the convective overshoot model, the contraction and ignition phases occur on a different timescale than they would in a "classical" core, calculated using the Schwarzschild criterion. It is this more extended contraction time and more powerful ignition that results in the "blue hook" morphology of the main sequence turnoff.

As evident from the displayed isochrone, the observational signatures of convective overshooting include an enhanced bend to the red of the main sequence turnoff, a blue hook structure to the very top of the main sequence resulting from a rapid evolution of turnoff stars to the blue, and a gap between the top of the main sequence and the subgiant branch. Such a gap is clearly evident near the top of the NGC 6819 main sequence at roughly $V = 14.6$ mag. We note that to securely reveal such a gap it is imperative that, in addition to removing non-members, binaries be identified and removed, since a binary population can mimic such a gap (e.g., Figure 5). It remains possible that the population of stars on the brighter side of the gap includes wider equal-mass binaries not identifiable by our spectroscopic techniques.

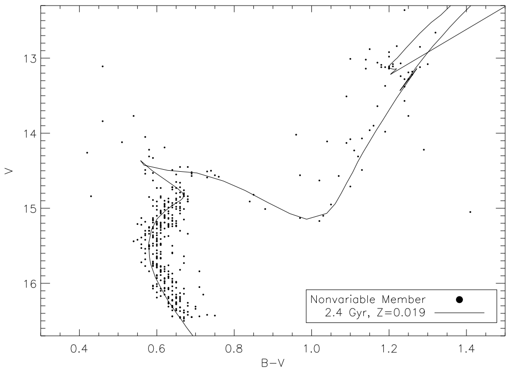

FIG. 6.— CMD showing only single narrow-lined cluster members. The cluster displays well-populated subgiant and giant branches and a population of single blue stragglers brighter and bluer than the cluster turnoff. The main sequence shows a marked bend to the red at the turnoff and a gap between the main-sequence turnoff and the subgiant branch. Also shown is an isochrone from the core convective overshoot models of Marigo et al. (2008) for reference. The turnoff morphology is fit well by the isochrone, and is characteristic of core convective overshoot.

Whether stars currently populate the blue hook itself is unclear because of confusion with the blue straggler population. Certainly there are stars in the NGC 6819 CMD consistent with populating the blue hook structure in the models. A study of the population density along the isochrone is merited to compare the expected and actual numbers. More detailed study of these stars may also allow identification of those that are blue stragglers, for example through differing rotation distributions.

7.2. *Stars of Note*

7.2.1. *Blue Stragglers*

We mark the location of candidate blue stragglers within the dotted lines in the bottom panel of Figure 5. This selection region is conservative, and does not include stars that could be currently populating the blue hook (either single stars or binaries), based on the isochrone fit of Figure 6 (see also Section 7.1). Likely there are more blue stragglers within the "notch" of the region.

Within this region we identify 12 candidate blue stragglers that are bluer and brighter than the cluster turnoff. We include here four stars that are to the blue of the turnoff, but somewhat fainter, as interesting candidates for future study.

It is generally accepted that blue stragglers are, or were, members of multiple systems whose evolution has been influenced by either stellar evolution or through dynamical processes resulting in mass transfer, mergers or even stellar collisions (e.g., Bailyn 1995). We note that only four of our potential blue stragglers currently display velocity variability (including the rapid rotator 014012), as opposed to the large frequency of binaries (∼75%) in the blue straggler population of the old (7 Gyr) open cluster NGC 188 (Geller et al. 2008). In Table 5 we list our data for these 12 NGC 6819 blue stragglers, in the same format as in Table 2.

TABLE 5
NGC 6819 Candidate Blue Stragglers

WOCS ID	α	δ	V	B-V	N_{WIYN}	N_{CfA}	$\overline{RV}$	Std. Err.	e / i	Mem. Prob.	Class	γ	Comment
009003	19 41 17.01	40 10 34.8	13.77	0.54	5	1	2.60	0.19	0.93	95	SM	···	···
014003	19 41 16.23	40 10 27.7	14.84	0.43	4	0	3.78	0.34	1.46	88	SM	···	···
009005	19 41 28.22	40 12 54.5	14.12	0.51	5	1	0.73	0.48	2.31	85	SM	···	···
010005	19 41 06.63	40 10 30.4	14.26	0.42	4	2	3.38	0.34	1.46	92	SM	···	···
005006	19 41 28.99	40 13 15.5	13.84	0.46	4	1	2.18	0.47	2.00	95	SM	···	···
016009	19 41 03.51	40 08 42.6	14.82	0.52	29	0	2.86	0.47	6.17	···	BLM	···	···
023011	19 40 54.75	40 08 35.5	15.44	0.54	6	0	2.45	0.12	0.66	95	SM	···	···
014012	19 41 17.01	40 06 04.0	14.84	0.47	10	0	1.52	1.87	···	···	BLM	···	Rapid rotator
007013	19 40 44.58	40 12 33.7	13.11	0.46	6	12	0.95	0.15	1.03	88	SM	···	···
010016	19 40 56.00	40 18 39.1	14.23	0.51	23	0	2.63	0.04	9.08	95	BM	2.408	SB1
003022	19 40 48.32	40 02 28.9	13.10	0.41	8	1	2.35	0.28	···	95	SM	···	Rapid rotator
032023	19 40 54.90	40 01 07.8	15.24	0.48	20	0	2.47	0.43	4.70	···	BLM	···	···

TABLE 6
NGC 6819 Candidate Red Clump Stars

WOCS ID	α	δ	V	B-V	N_{WIYN}	N_{CfA}	$\overline{RV}$	Std. Err.	e / i	Mem. Prob.	Class	γ	Comment
003002	19 41 21.99	40 12 02.1	12.76	1.12	2	32	1.04	4.48	···	···	BLM	···	Rapid rotator
004002	19 41 21.87	40 11 48.6	12.84	1.22	1	4	3.47	0.12	0.37	92	SM	···	···
005002	19 41 14.76	40 11 00.8	12.88	1.15	1	4	0.79	0.21	0.64	86	SM	···	···
006002	19 41 15.93	40 11 11.5	12.94	1.08	8	13	1.46	0.04	5.10	95	BM	2.190	SB1
008002	19 41 22.45	40 12 03.4	13.01	1.10	17	13	3.23	0.35	3.38	93	SM	···	···
009002	19 41 21.34	40 11 57.2	13.01	1.13	5	11	2.86	0.66	4.13	···	BLM	···	···
010002	19 41 13.55	40 12 20.6	13.06	1.17	1	4	2.37	0.23	0.70	95	SM	···	···
011002	19 41 13.45	40 11 56.2	13.12	1.18	5	3	2.96	0.08	0.41	94	SM	···	···
006003	19 41 12.79	40 12 23.9	13.12	1.19	1	4	2.79	0.05	0.16	95	SM	···	···
003005	19 41 29.54	40 12 21.0	13.07	1.23	6	4	2.72	0.10	0.57	95	SM	···	···
004005	19 41 21.48	40 13 57.3	13.08	1.21	15	3	1.50	0.32	2.81	93	SM	···	···
005005	19 41 08.59	40 13 29.9	13.11	1.21	1	4	2.00	0.21	0.64	95	SM	···	···
001006	19 41 17.76	40 09 15.9	12.84	1.11	4	13	1.68	1.04	6.48	···	BLM	···	···
002006	19 41 29.15	40 13 04.1	13.11	1.20	3	0	1.01	0.11	0.39	89	SM	···	···
002007	19 41 05.24	40 14 04.2	13.13	1.20	3	4	3.25	0.18	0.74	93	SM	···	···
003007	19 41 09.26	40 14 43.6	13.13	1.20	3	4	2.30	0.28	1.17	95	SM	···	···
003009	19 41 09.91	40 15 49.6	12.92	1.20	1	5	2.36	0.20	0.68	95	SM	···	···
004009	19 41 30.27	40 15 21.7	12.98	1.20	2	3	1.77	0.24	0.80	94	SM	···	···
006009	19 41 34.44	40 08 46.1	13.14	1.20	3	2	1.28	0.28	1.02	92	SM	···	···
003011	19 40 57.97	40 08 17.5	12.95	1.18	10	7	3.97	0.63	4.67	···	BLM	···	···
004011	19 40 50.20	40 13 11.0	13.09	1.18	1	3	3.26	0.32	0.86	93	SM	···	···
002012	19 41 16.32	40 05 50.9	13.11	1.20	13	6	3.73	0.04	6.20	95	BM	2.718	SB1
008013	19 41 02.03	40 06 28.1	13.14	1.14	3	4	2.56	0.09	0.39	95	SM	···	···
003021	19 41 23.86	40 21 44.5	13.02	1.14	7	0	1.74	0.07	0.45	94	SM	···	···

7.2.2. *Red Clump Stars*

We mark the approximate location of the red clump within the dashed rectangle (defined as $12.7 \lesssim V \lesssim 13.2$ and $1.06 \lesssim (B-V) \lesssim 1.23$) in the bottom panel of Figure 5. In Table 6 we list 24 potential red clump stars, and provide the same information as in our full RV database. Nearly one quarter (6/24) of the stars in the red clump are velocity variables. Five of these binaries likely have long periods (P > 500 days). The sixth, WOCS 003002, displays properties different from the rest and is worthy of particular attention.

003002: — The red clump binary 003002 has a circular orbit with a period of only 17.7 days. Such a short period is not expected for a binary with a primary star that has evolved through the tip of the giant branch and back to the red clump. Indeed, the current orbital separation would not permit a binary containing a star at the tip of the red giant branch without significant mass transfer and possibly a common-envelope phase.

On the other hand, the circular orbit would not be expected for a main-sequence non-member binary (e.g., Meibom & Mathieu 2005). Thus the circular orbit is additional evidence supporting 003002 being an evolved cluster member.

We suggest that the current state of the system may be the result of a dynamical encounter (or encounters). Such an encounter may have exchanged a more massive horizontal-branch primary star into the binary. This large-radius, deeply convective primary star would then rapidly circularize the orbit. Our preliminary investigations of this hypothesis show that this scenario is possible (Gosnell et al. 2007). We will discuss the likelihood of such an evolutionary history for 003002 in detail in a future paper.

8. CONCLUSIONS

In this paper we have described our high-precision radial-velocity study of solar-like stars within 23 arcmin square (13 pc) of the intermediate-aged open cluster

NGC 6819. We analyzed all available photometry and astrometry for the cluster in order to define a sample of candidate members, as reported in Table 1. We present the current results of our ongoing comprehensive RV survey of the cluster using the WIYN 3.5m telescope and the Hydra MOS. We supplement these RVs with an earlier CfA data set that, for some stars, significantly extends our time baseline, allowing us to detect and find orbital solutions for longer period binaries than would be possible with the WIYN data set alone. In Table 2 we show the combined RV database, including membership and binary status. The result of our work is a complete sample of all giants, subgiants and blue stragglers in the core of NGC 6819, as well as identification of a large, though not complete, sample of upper main sequence cluster members. Of these 480 cluster members, 83 appear to be hard binaries.

In § 7 we use our precise RV membership probabilities to construct a cleaned CMD of the cluster. Our analysis confirms the presence of core convective overshoot in the turnoff stars of the cluster, as indicated by the now evident morphology at the top of the main sequence. We identify a rich population of blue straggler cluster members, and list their properties in Table 5. Additionally, we list probable red clump members in Table 6. We also identify a binary in the red clump that, because of its short period of only 17.7 days, we conjecture is the product of a dynamical encounter.

In this survey we have shown the efficacy of RV measurements for unbiased surveys of open cluster membership, even when the cluster is rich, located within the plane of the Galaxy, and has a velocity distribution that is not entirely distinct from that of the field population. With this membership information in hand, NGC 6819 is ripe for further detailed analysis.

The WIYN Open Cluster Study will continue to study NGC 6819. In future papers, we will investigate the dynamical state of the cluster (e.g., mass segregation and velocity distribution) and provide the parameters for all binaries with orbital solutions, allowing us to study their distributions as well as to constrain the overall hard-binary frequency of the cluster. NGC 6819 is a benchmark intermediate-aged open cluster, and provides a critical constraint on the evolution of open clusters with rich binary populations.

The authors are grateful to the following individuals for invaluable contributions to this work: Joanne Rosvick and Jason Kalirai for providing their photometry data for our comparisons; Bob Davis, Jim Peters, Perry Berlind, Ed Horine, Joe Zajac and Ale Milone for their work on the CfA RV observations; Nigel Sharp for taking our original cluster photometry; Chris Dolan for initial setup work for the survey; and undergraduate and REU students Nick Stroud, Sylvana Yelda, Meagan Morscher, Michael DiPompeo and Natalie Gosnell. This research was funded in part by NSF grants AST-0406615 (R. D. M.) and AST-0406689 (I. P.). K. T. H. gratefully acknowledges support from the Wisconsin Space Grant Consortium and Oberlin College.

REFERENCES

Auner, G. 1974, A&AS, 13, 143

Bailyn, C. D. 1995, ARA&A, 33, 133

Barden, S. C., Armandroff, T., Muller, G., Rudeen, A. C., Lewis, J., & Groves, L. 1994, in Proc. SPIE Vol. 2198, p. 87-97, Instrumentation in Astronomy VIII, David L. Crawford; Eric R. Craine; Eds., 87

Bevington, P. R., & Robinson, D. K. 1992, Data reduction and error analysis for the physical sciences, 2nd edition (New York: McGraw-Hill)

Burkhead, M. S. 1971, AJ, 76, 251

Daniel, S. A., Latham, D. W., Mathieu, R. D., & Twarog, B. A. 1994, PASP, 106, 281

Friel, E. D., Liu, T., & Janes, K. A. 1989, PASP, 101, 1105

Geller, A. G., Mathieu, R. D., Harris, H. C., & McClure, R. D. 2008, AJ, 135, 2264

Glushkova, E. V., Kulagin, Y. V., & Rastorguev, A. S. 1993, Astronomy Letters, 19, 232

Gosnell, N., DiPompeo, M. A., Braden, E. K., Geller, A. M., & Mathieu, R. D. 2007, in Bulletin of the American Astronomical Society, Vol. 38, Bulletin of the American Astronomical Society, 839

Heggie, D. C. 1974, in IAU Symposium, Vol. 62, Stability of the Solar System and of Small Stellar Systems, ed. Y. Kozai, 225

Kalirai, J. S., et al. 2001, AJ, 122, 266, **(K01)**

Kang, Y.-W., & Ann, H. B. 2002, Journal of Korean Astronomical Society, 35, 87

Kirillova, T. S., & Pavlovskaya, E. D. 1963, Soviet Astronomy, 7, 99

Landolt, A. U. 1992, AJ, 104, 340

Latham, D. W. 1992, in ASP Conf. Ser. 32: IAU Colloq. 135: Complementary Approaches to Double and Multiple Star Research, 110

Lindoff, U. 1972, A&AS, 7, 497

Marigo, P., Girardi, L., Bressan, A., Groenewegen, M. A. T., Silva, L., & Granato, G. L. 2008, A&A, 482, 883

Mathieu, R. D. 1983, PhD Thesis, California Univ., Berkeley

Mathieu, R. D. 2000, in ASP Conf. Ser. 198: Stellar Clusters and Associations: Convection, Rotation, and Dynamos, 517

Mathieu, R. D., & Latham, D. W. 1986, AJ, 92, 1364

Mathieu, R. D., Latham, D. W., Griffin, R. F., & Gunn, J. E. 1986, AJ, 92, 1100

Mathieu, R. D., van den Berg, M., Torres, G., Latham, D., Verbunt, F., & Stassun, K. 2003, AJ, 125, 246

Meibom, S., & Mathieu, R. D. 2005, ApJ, 620, 970

Rosvick, J. M., & Vandenberg, D. A. 1998, AJ, 115, 1516, **(RV98)**

Sanders, W. L. 1972, A&A, 19, 155

Sandquist, E. L., Latham, D. W., Shetrone, M. D., & Milone, A. A. E. 2003, AJ, 125, 810

Sarrazine, A. R., Deliyannis, C. P., Sarajedini, A., & Platais, I. 2003, American Astronomical Society Meeting, 203

Shaviv, G., & Salpeter, E. E. 1973, ApJ, 184, 191

Skrutskie, M. F., et al. 2006, AJ, 131, 1163

Stefanik, R. P., Latham, D. W., & Torres, G. 1999, in Astronomical Society of the Pacific Conference Series, Vol. 185, IAU Colloq. 170: Precise Stellar Radial Velocities, ed. J. B. Hearnshaw & C. D. Scarfe, 354

Stetson, P. B. 1987, PASP, 99, 191

Street, R. A., et al. 2005, MNRAS, 358, 795

Street, R. A., et al. 2002, MNRAS, 330, 737

Street, R. A., et al. 2003, MNRAS, 340, 1287

Thogersen, E. N., Friel, E. D., & Fallon, B. V. 1993, PASP, 105, 1253

Tonry, J., & Davis, M. 1979, AJ, 84, 1511

van den Berg, M., Orosz, J., Verbunt, F., & Stassun, K. 2001, A&A, 375, 375

Vasilevskis, S., Klemola, A., & Preston, G. 1958, AJ, 63, 387

Zacharias, N., Urban, S. E., Zacharias, M. I., Wycoff, G. L., Hall, D. M., Monet, D. G., & Rafferty, T. J. 2004, AJ, 127, 3043

Zahn, J.-P. 2002, in Astronomical Society of the Pacific Conference Series, Vol. 259, IAU Colloq. 185: Radial and Nonradial Pulsations as Probes of Stellar Physics, ed. C. Aerts, T. R. Bedding, & J. Christensen-Dalsgaard, 58